Inverse Problems and Imaging doi:10.3934/ipi.2021015

LARGE REGION INPAINTING BY RE-WEIGHTED REGULARIZED METHODS

Yiting Chen, Jia Li* and Qingyun Yu

School of Mathematics, Sun Yat-Sen University
135 Xin Gang Xi Lu
Guangzhou, 510275, China

(Communicated by Tieyong Zeng)

Abstract. In the development of imaging science and image processing request in our daily life, inpainting large regions always plays an important role. However, the existing local regularized models and some patch manifold based non-local models are often not effective in restoring the features and patterns in the large missing regions. In this paper, we will apply a strategy of inpainting from outside to inside and propose a re-weighted matching algorithm by closest patch (RWCP), contributing to further enhancing the features in the missing large regions. Additionally, we propose another re-weighted matching algorithm by distance-based weighted average (RWWA), leading to a result with higher PSNR value in some cases. Numerical simulations will demonstrate that for large region inpainting, the proposed method is more applicable than most canonical methods. Moreover, combined with image denoising methods, the proposed model is also applicable for noisy image restoration with large missing regions.

1. **Introduction.** Image inpainting, initially introduced to digital image processing by [3], is about recovering the damaged pixels or regions from the corrupted image. It often comes with the missing of image pixels, erasing unwanted objects of the image, or the recovery of the degraded image damaged by various means. For example, when restoring old photographs, the broken holes or spots of them need to be repaired; or sometimes it needs to remove the disturbing targets of a processed image such as the words, scratches or marks added by people. Good recovery of the damaged regions should have clear features such as edges, textures and consistent smoothness, and less unnatural noise or artifacts. After restoration, the boundary between the damaged regions and the reliable parts usually should not be a sharp edge of the new image.

The goal of image inpainting simply can be described as recovering a clear image u from the initial corrupted image f. We represent the image as a matrix in $\mathbb{R}^{m\times n}$, where $m\times n$ is the size of the digital image. Mathematically, the model for inpainting can be summarized as follows:

$$f(x) = \begin{cases} u(x), & x \in \Lambda \\ v(x), & x \in \Lambda^c \end{cases}, \tag{1}$$

2020 *Mathematics Subject Classification.* Primary: 65D18, 68U10; Secondary: 65J22.

Key words and phrases. Image inpainting, non-local regularization, re-weighted regularization.

The corresponding author's work is partially supported by NSFC young researchers' grant 11801594 and Guangdong-Hong Kong-Macau Applied Math Center grant 2020B1515310011.

* Corresponding author: Jia Li.

where f is the corrupted image, u is the original image we want to estimate, Λ is the index of the observed valid pixels. v represents the value of pixels of the inpainting domain and it can represent a diversity of damaged types of image. For instance, v is a zero matrix if the information of the inpainting region loses completely, while v is the unwanted patterns of the observed image when we are trying to remove them.

In early literature, the image inpainting is mainly based on filter-based models [3, 4], in which the Criminisi method [17] has better performance because of its inpainting order and edge preservation. Later on, some variational based regularized methods or wavelet frame [36, 20] regularized methods [15, 16, 13, 8, 14, 9, 29] have even better performance in generating smooth regions and sharp edges. Moreover, from the technique of simultaneous cartoon and texture restoration [23], Cai et.al. proposed a two-system wavelet frame regularized method [10], which helps preserve textures in the smooth regions. [19] proposed a blind-inpainting method for the cases where the inpainting index set Λ^c is unknown and cannot be accurately detected. In summary, the above wavelet frame based models are based on local regularization, which has not considered the similarity from different positions in an image. In practice, however, when the missing region is slightly larger or the scratch line is bolder, the local regularization, mainly recovering the missing pixels by neighborhood information, cannot accurately estimate the brightness of missing pixels . Therefore, it is necessary to recover the missing/damaged pixels from non-local information via patch matching [6, 7, 18], which contributes to discovering and enhancing the non-local repetitive patterns. Nevertheless, their models are still lack of integrity. For instance, [2, 31, 21] introduced some variational based non-local inpainting methods. In particular, [31] proposed a universal variational framework (UVF) for non-local inpainting and has better performance for inpainting with less proportion of Λ. The above regularized models are based on various linear/non-linear functions of non-local partial derivatives of images, such as the non-local gradient $\nabla_{NL} f$, where f is the object inpainted image. Additionally, [5] introduced a Coherence Transport based Non-Local inpainting methods (CTNL) and [32] provided an upgraded method with adaptive distance functions. [24] introduced a dictionary learning based method and [22] introduced the bilateral variance estimation for non-local image restoration, considering both the similarity of patches and the distance between patches. Compare with the non-local regularized models, these statistical methods proposed non-local regularizations that may be more agree with the similarities of non-local patches in most natural images.

In recent years, based on computational differential geometry, there were some works on inpainting problems, such as Manifold based Low-Rank regularized (MLR) method [30], Low-Dimensional Manifold Method (LDMM) with/without Weighted Graph Laplacian (WGL) [34]. Simultaneously, Newson et.al. proposed a non-local patch based (NLPB) method [33], which is beneficial for improving the quality of small region inpainting and texture preservation. However, in some practices, they showed great inadaptability when the inpainting domain is very large, i.e. the diameter of the inpainting region is over 50 pixels or several times of the patch size. As the results illustrated in FIG 1.1, both the UVF non-local method [31] and the MLR method [30] generate meaningless regions without any valuable information. At the same time, the Criminisi method [17], CTNL method [32], LDMM+WGL method [34] and the NLPB method [33] generate some features similar as the boundary of grapes but also generate lots of unnatural artifacts (either too blurry or too sharp).

In this situation, it is difficult to construct the inner part from merely the single image f due to the severe loss of information. There are some machine learning and big data based methods, such as a generative image inpainting method [38], to deal with the large region inpainting in some case. But the models are usually much more time and memory-consuming and intensely sensitive to the amount and quality of the training data.

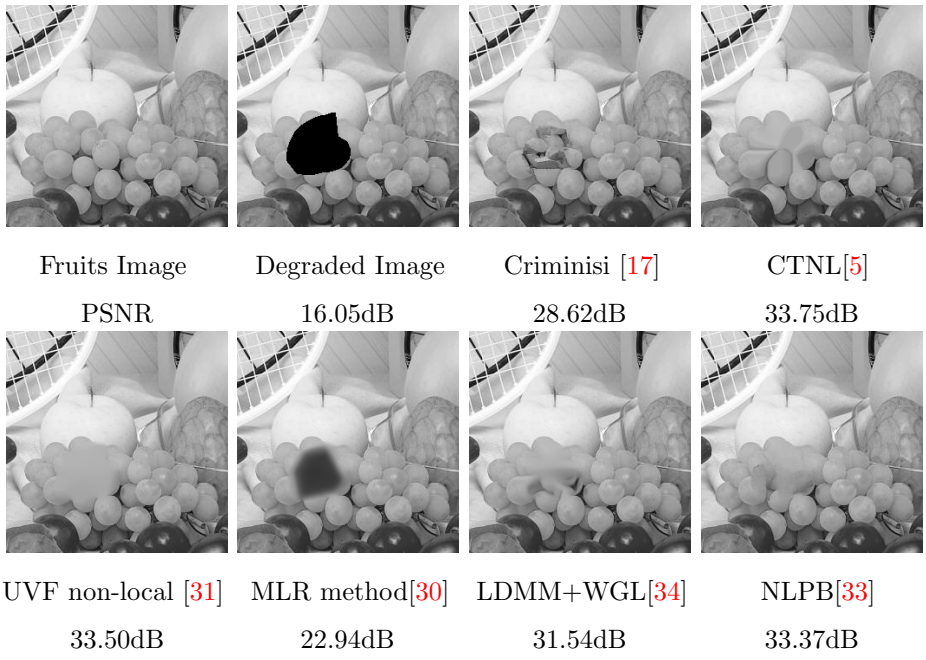

FIGURE 1. Large region ipainting by some canonical and recent methods.

In this paper, based on the non-local patch matching scheme, we will first propose that it is effective to inpaint from outside to inside when the inpainting region is large. By such a strategy, the outer part of the large region can be estimated without the interference of the unknown inner part, while the inner part can be estimated after a reasonable outer part has been restored. Furthermore, we will propose a re-weighted matching algorithm by closest patch (RWCP) and another re-weighted matching algorithm by distance-based weighted average (RWWA). Both re-weighted methods are based on iterative algorithms and dynamical weight in the regularized model, reflecting the strategy of inpainting from outside to inside. In numerical simulations, by different regularization terms, the proposed RWCP model can recover clearer features while the RWWA model can construct a relatively smooth and reliable pattern. Compared with other recent methods, our proposed re-weighted models can reconstruct more reasonable features in the large and inpainting region. This means the restored image looks natural and cannot be recognized as an inpainted image at a short glance. Moreover, for almost all inpainting cases, our proposed re-weighted models have the highest PSNR value, which fully guarantee the inpainting accuracy. Additionally, we will demonstrate that the proposed models can be combined with denoising methods when restoring noisy images with large missing regions. Therefore, this paper would provide a novel non-local patch

matching based method that is most applicable for large regions inpainting from single degraded image.

The rest of this paper will be organized as follows. In Section 2, we will propose a benefit inpainting order and two re-weighted models for image inpainting. They help recover more features of the image with or without Gaussian noise. We will implement numerical experiments and compare with the popular methods in Section 3. In Section 4, we will give a brief conclusion of our work.

2. Proposed models.

For inpainting large regions, the canonical mean, median filter-based method [3], or existing regularized methods [12, 9, 10, 37, 30] cannot accurately estimate the inner part of the missing large region. Due to the difficulties in utilizing the neighborhood information or directly formulating patches to estimate the inner part, it is natural to finish the inpainting from the boundary to the center of the missing region.

2.1. Non-local inpainting from outside to inside.

Generally speaking, all regularized image inpainting model can be summarized as follows:

$$\min_u \sum_{x\in\Lambda^c} R_x(u) \quad s.t. u|_\Lambda = f|_\Lambda, \tag{2}$$

where u is the estimated image, f is the degraded image, Λ is the index set for available pixels such that $f|_\Lambda$ is the same as the ground truth in Λ, Λ^c is the complement set representing the missing pixels. The operator $R_x(u)$ is a non-local regularization operator that defines the similarity of the pixel centered at pixel x and its similar pixels. In early literature, the non-local regularization operator $R_x(u)$ can be constructed by a simple difference of patches (such as (3) or see [6, 25]), which reduces the difference with similar and nearby patches. In recent literature, $R_x(u)$ can also be defined as the patch manifold regularization operators proposed in [37, 30]. For different settings of $R_x(u)$, the solution of u can be solved by either direct solve the linear combination of valid intensities or iterative algorithms, such as the Alternating Direction Method of Multipliers (ADMM) [28]. In practice, however, when the diameter of the missing region is much larger than the patch size, then the above regularization operators $R_x(u)$ usually generate the solutions with a sizeable blurry region without any useful information. Therefore, it is necessary to provide a strategy to restrict the order of inpainting, such as inpainting from outside to inside. The representation of local patches with similarity can be illustrated as in FIG. 2. In literature, the inpainting from outside to inside has appeared in a coherent based method [32] and the non-local patch based method [33]. One is based on the contour of a skeleton function while the other relies on the weight function. In this paper, we will utilize the similarity of non-local patches and inpaint from outside to inside by different approaches.

Consider the patch $P(x)$ centered at the pixel x, if we take the regularization term $R_x(u)$ as the square of Frobenius norm between the most similar patches, the definition can be given as:

$$R_x(u) = \min_{P(y)\subset\Lambda} \sum_{t\in\Lambda\cap P(x)} (u(t) - f(t+y-x))^2. \tag{3}$$

where $P(y)$ is the patch centered at another pixel y and fully contained in the set Λ. In fact, during the inpainting procedure, it is relatively easier to estimate the boundary part of the missing region whose accurate neighborhoods are more than

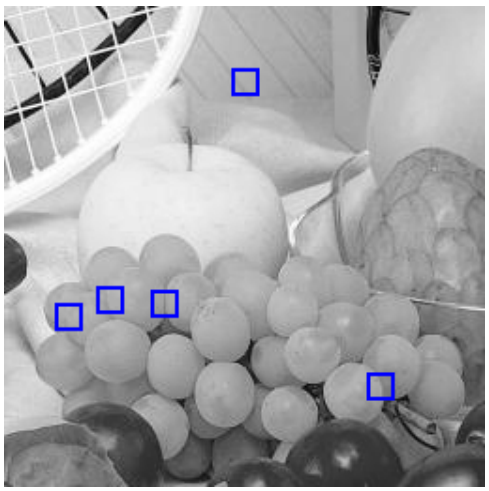

FIGURE 2. An example of similar patches in fruits image.

the inner part. Therefore, one can first inpaint these boundary pixels by a non-local matching method. Then the inner part of the missing region can be estimated with more reasonable patterns or features rather than a blurry part. To emphasize the importance of this inpainting scheme, we first estimate each pixel x by minimizing $R_x(u)$ defined in (3), respectively. All the non-local matching is based on the matching between the unknown patches and full accurate patches, accounting for a simple inpainting scheme. The importance is to calculate the geometric center of the large missing regions and define the order of inpainting. These details of the simple inpainting algorithm from outside to inside can be stated as in Algorithm 1. In Section 3, FIG. 5 shows that even such a simple algorithm helps protect some features in the large region for inpainting, implying that an inpainting scheme from outside to inside is applicable and effective for large region inpainting.

Algorithm 1 Strategy of re-weighted inpating for large region

Step 0. Calculate geometric center of the missing region x_c (the choice is not sensitive and can be simply defined as the median of the coordinates for all missing pixels if the missing regions are convex or nearly convex). Then sort the missing pixel set Λ^c by the distance to the geometric center x_c. Denote the sorted set Λ^c as a sequence $\{x_k\}_{1\leq k\leq L}$, where L is the cardinality of Λ^c. Initialize i as $i = 1$.
while $i \neq L$ **do**
Step 1. For each x_i, estimate the brightness u_{x_i} by minimizing $R_x(u)$ defined in (3).
Step 2. Set x_i in Λ, x_i out of Λ^c, $f_{x_i} = u_{x_i}$
Step 3. Set $i = i + 1$.
end while

2.2. **Re-weighted Model.** Generally speaking, the above inpainting strategy simply restricts the inpainting order and improves the quality of the inpainting of the large regions. However, such a strategy only builds up weak connection between the

unknown pixels, which is generally focused on most non-local models in the literature. In this paper, we mainly propose a re-weighted algorithm, which is essentially a different approach of solving (2) with iterative strategy and a particular inpainting order. The re-weighted model for each iteration can be defined as follows:

$$\min_u \sum_{x\in\Lambda_i^c} R_{x,W_x}(u) \quad s.t. u|_{\Lambda_i} = f|_{\Lambda_i}, \tag{4}$$

where Λ_i is the reliable pixel set in i-th iteration that initially equals to Λ and would finally equal to the whole image set Ω. For each unknown pixel x, $R_{x,W_x}(u)$ is the re-weighted regularized operator whose weights in different pixels are different. The weight W_x for pixel x is between 0 and 1, representing the reliability of each pixel x. During the i-th iteration, the reliable set Λ_i and all weight matrices $\{W_x\}$ are fixed therefore the definition of $R_{x,W_x}(u)$ is similar to the non-weighted regularization term $R_x(u)$. To simulate the strategy of inpainting from outside to inside, the weight W_x should be larger for boundary pixels and smaller for inner pixels of the missing region. During the iterations, the weights W_x keeps increasing and the weight at the boundary pixels of missing regions are always relatively higher, which implies that the boundary part can be estimated earlier and can be utilized to inpainting the inner region. Therefore, the algorithm has a similar strategy as (2) but can update the brightness in Λ^c several times. Therefore, the only problem is how to define the dynamical index set Λ_i and the weight matrices $\{W_x\}$.

In this paper, the value of W_x is always 1 if the pixel x is in Λ, which means the valid pixels can always be fully trusted. The other weights W_x for $x \in \Lambda^c$ varies from different iterations if the pixel is in Λ^c. For pixels in Λ^c, the itinial weights are 0, and keep increasing during the iterations. After each iteration, for the pixels near the boundary of inpainting region with weights higher than a threshold value T, we set it as 1 and assume the inpainting of the pixel is finished, while other weights for inner pixels in Λ^c would be updated by the average of neighborhood's weights that are also increased if it is near the boundary. In the meantime, we define an expanding available set Λ_i that includes more and more pixels from outside to inside. As a result, the weights increase and the Λ_i expands to the whole set Ω, and the algorithm will stop and converge in a few iterations. In this paper, the threshold parameter T is set as an empirical value 0.6 and the result of inpainting is not sensitive to T if it is between 0.4 and 0.8. The detail of the re-weighted strategy is stated as Algorithm 2.

Theoretically, when all the weights W_x tend to 1, the ultimate solution of Algorithm 2 should have a similar result as that from Algorithm 1. But surprisingly, such a strategy can make the algorithm more likely to converge to a solution with clear regions and features in Λ^c. The reason can be explained as that the index set Λ_i explodes during iterations. Moreover, the re-weighted system gives higher initial weights at the boundary part and lower weights in the inner part of the missing region. Therefore, the boundary part can be estimated earlier and the inner part can be ignored without confusing the boundary part. After the boundary part has been estimated and joined the set Λ_i, the inner part of the missing region can be estimated from all other pixel values. Then the inpainting region can be regarded as smaller. Therefore, it is natural to understand that Algorithm 2 as an upgrade of the simple inpainting Algorithm 1.

In practice, similar to (3), the regularization term $R_{x,W}(u)$ can be similarly defined by the difference between the closest patch . The main difference is caused

Algorithm 2 Strategy of re-weighted large region inpating

Step 0. For each pixel $x \in \Omega$, set initial weight $W_x = \begin{cases} 1, x \in \Lambda \\ 0, \text{otherwise} \end{cases}$. Denote $\Lambda_1 = \Lambda, \Lambda_1^c = \Lambda^c$. Set the threshold parameter $0 < T < 1$ for sufficiently reliable of each pixel during the inpainting, which means when $W_x > T$ the pixel can be fully trusted and the inpainting is finished. Set the initial value i as $i = 1$.
while $\Lambda_i \neq \Omega$ **do**
  Step 1. Solve the model (4) with fixed weight W_x by direct non-local matching method or ADMM algorithm [28], and update the solution of u.
  Step 2. For each pixel $x \in \Lambda_i^c$, calculate the temporary weight as the average weight $\mathcal{W}_x = \frac{\sum_{y \in P(x)} W_y}{Patchsize^2}$ in the patch centered at x. $Patchsize$ is always set to be 11 for this paper. This step makes the weights keep incerasing, with outside weights converges to 1 earlier while the inner weights converges to 1 later.
  if $\mathcal{W}_x > T$ **then**
    Set x in Λ_{i+1}, $f_x = u_x$, set the weight $\mathcal{W}_x = 1$.
  else
    Set x in Λ_{i+1}^c.
  end if
  Step 3. Set the updated weight $W_x = \mathcal{W}_x$ for all the pixels x.
  Step 4. Set all pixels in Λ_i in Λ_{i+1}.
  Step 5. Set $i = i + 1$.
end while

by the weight W_t at each pixel, resulting in that the pixels with higher weight, or reliability would be considered heavily. We define as follows:

$$R_{x,W}(u) = \min_{P(y) \subset \Lambda_i} \sum_{t \in P(x)} W_t \cdot (u(t) - u(t + y - x))^2, \tag{5}$$

where $P(y)$ centered at y are other pixels for comparing with $P(x)$, t represents the position of different pixels in $P(x)$. When the regularization term (5) is applied, the algorithm tends to duplicate the closest patch to the unknown region. In Algorithm 2, since the inner part has lower initial weights and the outer part has higher weights, the object function would be mainly determined by pixels at the boundary part of the inpainting region, similar to the strategy of inpainting from outside to inside. When the iteration converges, all the weights W_x tend to 1 the model (4) would tend to the model without weight. The solution is slightly better than that in Algorithm 1 and it is generated by an iterated model strictly.

Sometimes in practice, regularization term (5) can easily cause overfitting, hence we also propose another Gaussian weighted distance-based regularization term as:

$$R_{x,W}(u) = \sum_{P(y) \subset \Lambda_i} \exp\left(-\frac{\sum_{t \in P(x)} W_t \cdot (u(t) - u(t + y - x))^2}{\sigma^2} \right) \cdot (u(x) - u(y)), \tag{6}$$

where the parameter σ is always set as constant 500 in all the numerical simulations. Following this paper, we call Algorithm 2 with regularization term (5) as Re-weighted matching algorithm by closest patch (RWCP). Besides, we call Algorithm 2 with regularization term (6) as Re-weighted matching algorithm by distance-based weighted average (RWWA). We will show that both methods have

their unique superiority in numerical simulations. In particular, the regularization term (5) performs the best visual quality for almost all simulation.

The following FIG. 3 shows that as an example of inpainting the fruits image in FIG. 1, the object functions for both our proposed RWMC and RWWA model converge fast to their minimum values.

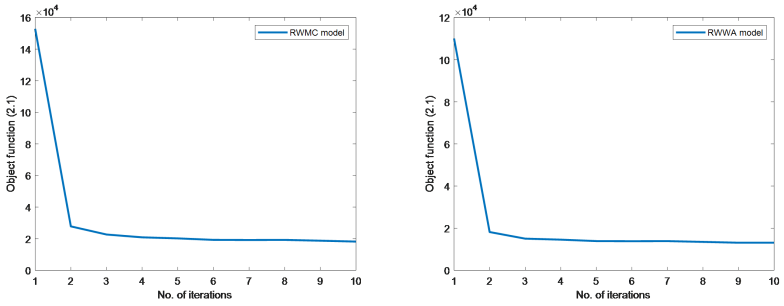

FIGURE 3. Convergence curve for the object functions in Algorithm 2. The left image is the convergence curve for RWMC model and the right image is that for RWWA model.

2.3. **Image inpainting from noisy image with large missing region.** In practice, some images might include some large missing/damaged regions, at the same time, the rest pixels are also corrupted by additive noise such as Gaussian noise. Therefore, we also discuss the model for large regions inpainting from noisy images. In literature, image denoising technique has been improved from local regularized models [27, 26] to non-local regularized and dictionary learning based models [6, 18, 1, 11]. In recent years, image denoising can be efficiently performed by some pre-trained neuron networks, such as Denoise Convolutional Neural Network (DnCNN) [39].

When the degraded image f has a large region $\Omega\backslash\Lambda$ to be inpainted, it is necessary to decide the order of removing the noise and inpainting the missing region. It can be naturally observed that if the inpainting is based on a denoised image, the original information might be smoothed or lost. On the other hand, the large region would be noisy if the inpainting is directly based on noisy prior knowledge. To deal with this dilemma, this paper proposes a two-stage algorithm to inpaint a noisy full image, in which the outer part of the large region can be trusted with edges and features while the inner part is slightly not acceptable. Then we rectify the inner part of the inpainted regions with lower weight by more iterations of Algorithm 2 after the denoising. The detail of the algorithm is shown in Algorithm 3.

It can be clearly seen in FIG. 4 that "Denoise and Inpaint" scheme may easily generate artifacts so that the boundary of the large region can be clearly observed with artifacts. On the other hand, "Inpaint and Denoise" scheme generates a smoother image while the inner part of a large region is over smoothed and blurred. Compared to the previous two schemes, Algorithm 3 has the best result in terms of both the visual quality and the PSNR value.

3. **Numerical results.** In this section, we implement numerical simulations for our proposed inpainting algorithms for image inpainting from missing large regions.

Algorithm 3 Strategy of re-weighted large region inpainting from noisy images

Step 1. From the noisy image f with missing region, inpaint the large region by ONLY ONE ITERATION of Algorithm 2 with RWCP regularization term to formulate a full noisy image u_1.
Step 2. Using a denoising method to u_1 (such as DnCNN based denoising proposed in [39]) to remove the noise and generate a clear image u_2.
Step 3. Inpaint the inner part of the large region with weight less than $T = 0.6$ by implementing more iterations of of Algorithm 2 with RWCP regularization to estimate a clear image u_3.
Step 4. Using the denoising method again to u_3 to generate an ultimate estimation of clear image u.

Noisy Fruits Image	Denoise & Inpaint	Inpaint & Denoise	Algorithm 3
15.81dB	30.63dB	30.81dB	31.12dB

FIGURE 4. The result of large region inpainting from noisy images with Gaussian noise $\sigma = 10$.

Our results validate that the proposed methods can inpaint the large region by accurate, similar or at least reasonable patterns. In contrast, most other existed models can only generate images with unacceptable visual observation by either blurry regions or some artifacts. In practice, some results may have lower error but they include large blurry inpainted parts. Therefore, for all image restoration results, we mainly focus on the visual quality and comfortableness to see whether the region has more clear features and fewer artifacts. As a minor consideration, we also quantitatively evaluate the restoration error by peak signal-to-noise ratios (PSNR) value:

$$\mathrm{PSNR}(f, \tilde{f}) = 10 \log_{10} \frac{MN(f_{\max} - f_{\min})^2}{\|f - \tilde{f}\|_2^2},$$

where $\tilde{f}$ is the ground truth image, $f_{\max}$ and $f_{\min}$ are its maximal and minimal pixel values respectively and M, N represent the size of the image.

In practice, the quality of inpainting is always determined by the features of restored images and the numerical error to the ground truth images. Generally speaking, for most natural images, our proposed re-weighted RWCP method always has the best performance in visual quality which makes the result images "natural and difficult to be recognized as an inpainted image". On the other hand, our proposed RWWA method sometimes has an even higher PSNR value, implying the least relative error to the ground truth image. FIG. 5 shows that for the fruit's image, the local wavelet frame-based model [35, 9] and the UVF non-local model [31] can only reconstruct a blurry region without any information though high

PSNR value. The Criminisi method [17] generates a lot of artifacts without smooth grape regions. The MLR method in [30] fails to estimate the inner part of the missing large region and only gives a gray part. The low dimensional manifold + weighted graph Laplacian method (LDMM+WGL) [34] and CNTL method [32] has the partial blurry part and partial artifacts part with the shape not similar to grapes. Conversely, our proposed simple directional inpainting Algorithm 1 can provide a reasonable inner region that looks like some shape of grapes. Its result is comparable to the result from NLPB method [33]. Furthermore, our proposed re-weighted model with the closest patch regularization term (RWCP) provides the highest PSNR value and can reconstruct an even clearer region including several precise shapes and boundaries of grapes. Another proposed re-weighted model with distance-based average regularization term (RWWA) can also generate a clear outer part of the missing region and there are almost no artifacts in the restored image. Compared to other existed methods, our methods are more applicable for such inpainting problem from large missing regions.

For other numerical simulations, there are two examples for boat image with smaller inpainting region in FIG. 6. Compared to two recent methods, LDMM+WGL [34] and NLPB [33], our proposed RWCP method recovers more features and generates fewer artifacts. For example, only the RWCP method recovered a clear and sharp "ship tail" structure, hardly recognized as "inpainted". Moreover, for "Fingerprint" image and "Bricks" image with more textures, the RWCP method has a definite advantage in terms of visual quality and PSNR value. Although the NLPB method [33] also duplicates some reasonable features in the inpainting region, the curves at the boundary are discontinuous, apparently reducing the reliability of the inpainting. On the other hand, our proposed RWWA method has the highest PSNR value for "Boat 1" and "Fingerprint" image, which shows that the features for these results are most reliable although parts of the inpainting region is still blurry. Furthermore, by Canny edge detection operator, FIG. 7 also indicates that the RWCP method recovered most valid edges, textures or features with almost no artifacts in the large missing domain. In contrast, the LDMM+WLG [34] and NLPB [33] have a larger hole without edges and textures or generate some unnatural singularities. Therefore, we can claim that for large domain inpainting from the single degraded image, the proposed methods have a better utilization in non-local matching, bringing results with more sharp edges and reliable features.

Additionally, we simulated the proposed Algorithm 3 for large regions inpainting from noisy images with different levels of Gaussian noise. FIG. 8 shows that Algorithm 3 is applicable for inpainting noisy images with large missing regions, which has not and could not be solved by most existing single image restoration methods.

4. **Conclusion.** In this paper, we first proposed Algorithm 1 as a simple image inpainting model by non-local matching and strategy of inpainting from outside to inside. With the demonstration and comparison in FIG. 5, we elaborate that such a simple inpainting strategy is applicable and effective for large region inpainting. However, Algorithm 1 cannot update and improve the inpainting region so that such an algorithm still generates some unnatural artifacts. Therefore, the proposed re-weighted models RWCP and RWWA can further solve such issues, generating the result with more reasonable features, fewer artifacts, and higher inpainting accuracy. FIG. 5 and 6 show that for various types of large region inpainting, our proposed models always outperform the existing local wavelet regularized model [9], the LDMM+WGL method [34], and the MLR method [30] which are totally

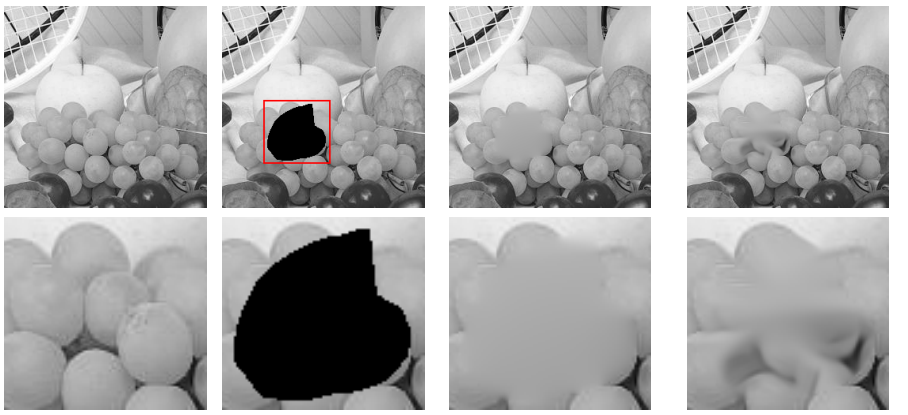

Fruits Image | Degraded Image | Wavelet Model [9] | LDMM+WGL [34]

PSNR | 16.05dB | 34.10dB | 31.54dB

MLR method [30] | Criminisi [17] | CNTL [32] | UVF non-local[31]

22.94dB | 28.62dB | 33.75dB | 33.50dB

NLPB[33] | Algorithm 1 | RWCP | RWWA

33.37dB | 32.72dB | 34.50dB | 34.16dB

FIGURE 5. Large region inpainting for a fruits image.

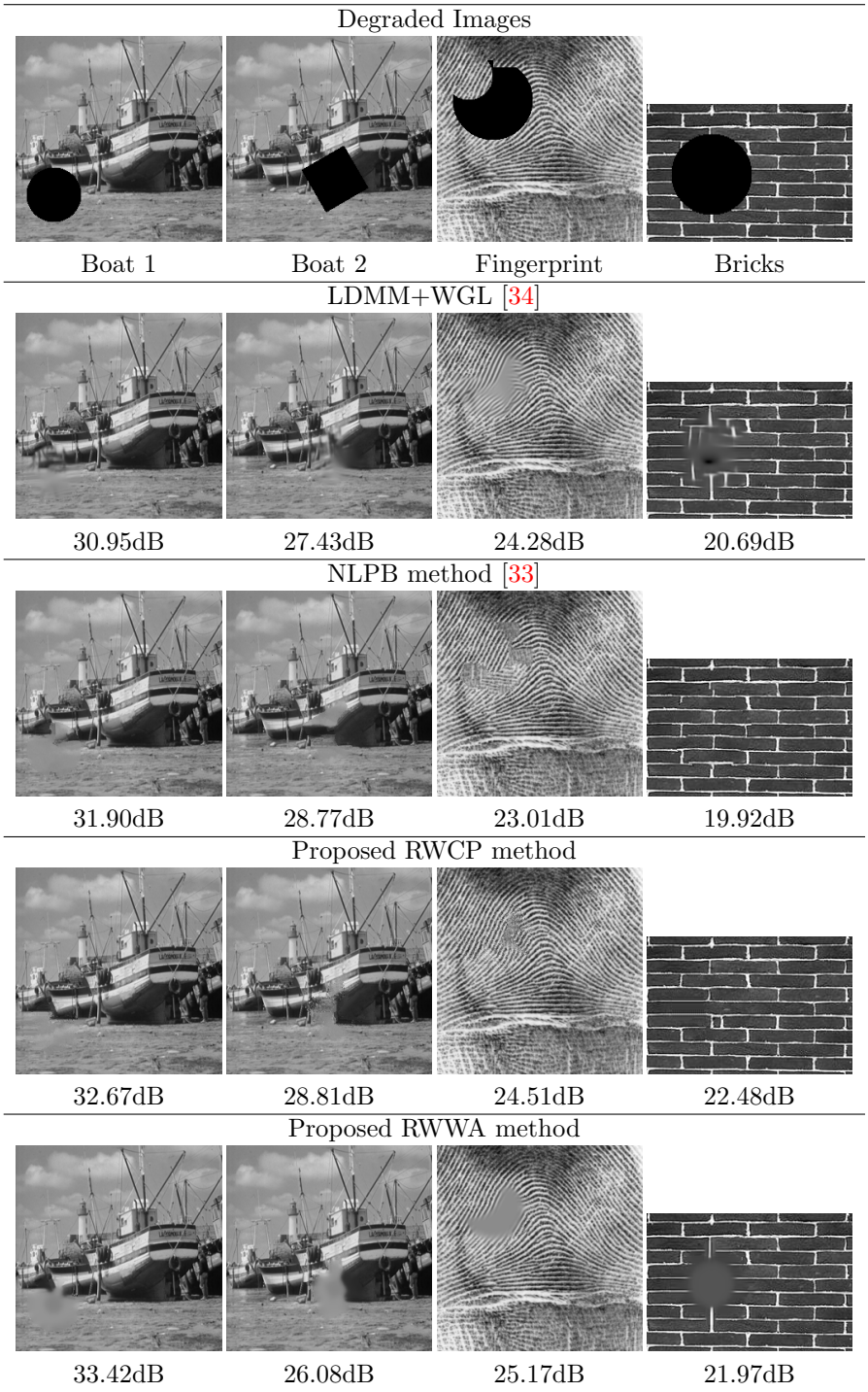

FIGURE 6. Numerical results for boat and bricks image inpainting from missing large region.

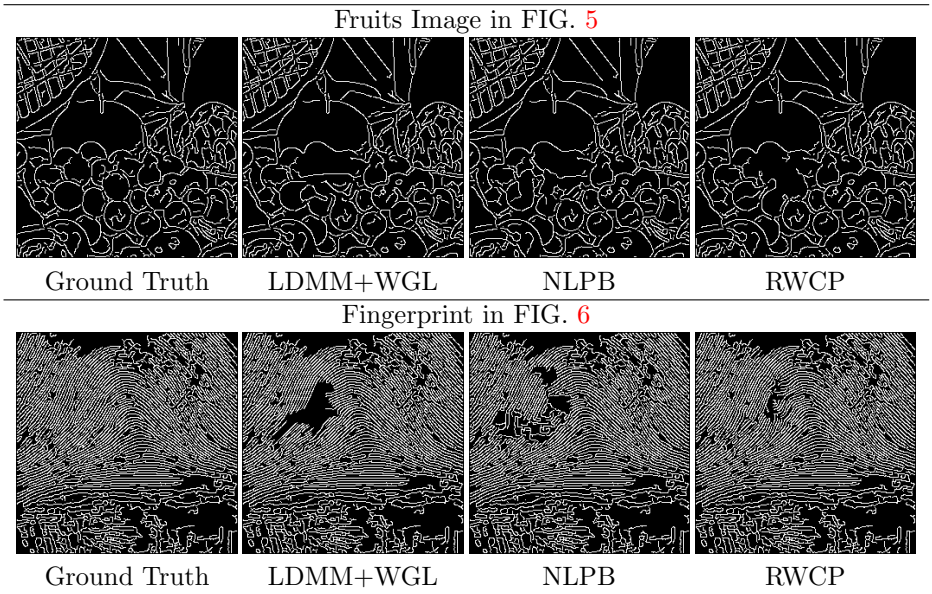

FIGURE 7. Edge detection of inpainting results via Canny operator.

not applicable for large domain inpainting. Furthermore, FIG. 8 shows that by the appropriate composition of the proposed large region inpainting method and image denoising method, it is possible to restore clear images from noisy images with large missing regions. The strategy, models, algorithms, and results of this paper can be applied to other large domain inpainting or restoration problems. From this paper as a new example, the non-local matching was validated as still an essential scheme for image restoration from single images. In the future, the result of this paper can also be compared or combined with the big-data or deep learning based image inpainting methods.

Acknowledgments. We first thank all the editors and reviewers for the supporting and improving of this paper. We thank Dr. Rongjie Lai and Dr. Zuoqiang Shi for sharing their code of MLR and LDMM+WGL methods. We also thank Ms. Sisi Gai, Mr. Dongrong Li, Ms. Li Lin and Mr. Duo Zhang for their help in result evaluation and parameter tuning.

REFERENCES

[1] M. Aharon, M. Elad and A. Bruckstein, An algorithm for designing overcomplete dictionaries for sparse representation, *IEEE Transactions on Signal Processing*, **54** (2006).
[2] P. Arias, V. Caselles and G. Sapiro, A variational framework for non-local image inpainting, **08** (2009), 345–358.
[3] M. Bertalmio, G. Sapiro, V. Caselles and C. Ballester, Image inpainting, *Siggraph'00*, (2000), 417–424.
[4] M. Bertalmio, L. Vese, G. Sapiro and S. Osher, Simultaneous structure and texture image inpainting, *IEEE Transactions on Image Processing*, **12** (2003), 882–889.
[5] F. Bornemann and T.äMrz, Fast image inpainting based on coherence transport, *Journal of Mathematical Imaging & Vision*, **28** (2007), 259–278.
[6] A. Buades, B. Coll and J.-M. Morel, A non-local algorithm for image denoising, in *2005 IEEE Computer Society Conference on Computer Vision and Pattern Recognition (CVPR'05)*, **2** (2005), 60–65.

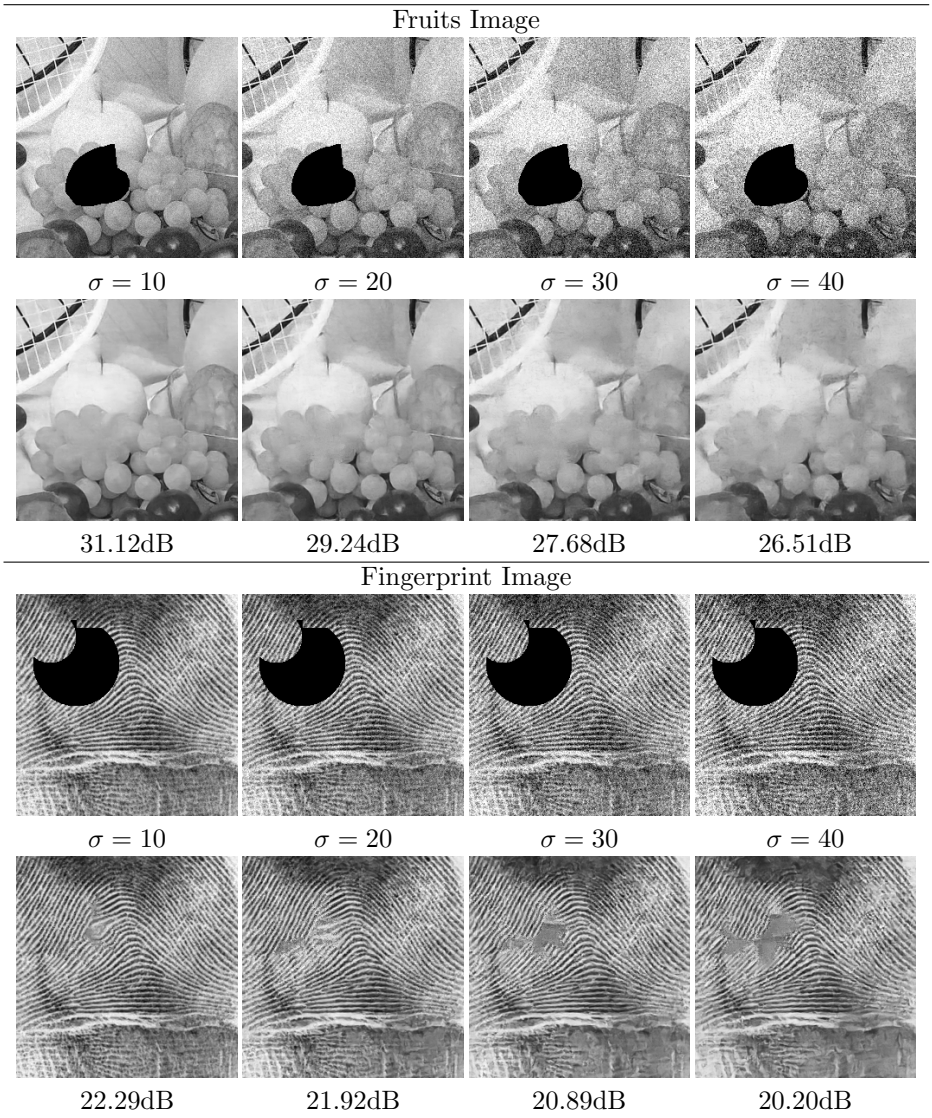

FIGURE 8. Large region inpainting from images with Gaussian noise by Algorithm 3.

[7] A. Buades, B. Coll and J.-M. Morel, Image enhancement by non-local reverse heat equation, Preprint CMLA, **22** (2006), 2006.
[8] J.-F. Cai, R. H. Chan, L. Shen and Z. Shen, Convergence analysis of tight framelet approach for missing data recovery, *Advances in Computational Mathematics*, **31** (2009), 87–113.
[9] J.-F. Cai, R. H. Chan and Z. Shen, A framelet-based image inpainting algorithm, *Applied and Computational Harmonic Analysis*, **24** (2008), 131–149.
[10] J.-F. Cai, R. H. Chan and Z. Shen, Simultaneous cartoon and texture inpainting, *Inverse Probl. Imaging*, **4** (2010), 379–395.
[11] J.-F. Cai, H. Ji, Z. Shen and G.-B. Ye, Data-driven tight frame construction and image denoising, *Applied and Computational Harmonic Analysis*, **37** (2014), 89–105.
[12] R. Chan, L. Shen and Z. Shen, A framelet-based approach for image inpainting, *Research Report*, **4** (2005), 325.

[13] T. F. Chan, S. H. Kang and J. Shen, Euler's elastica and curvature-based inpainting, *SIAM Journal on Applied Mathematics*, **63** (2002), 564–592.
[14] T. F. Chan and J. Shen, *Image Processing and Analysis: Variational, PDE, Wavelet, and Stochastic Methods*, Society for Industrial and Applied Mathematics (SIAM), Philadelphia, PA, 2005.
[15] T. F. Chan and J. Shen, Variational image inpainting, *Commun. Pure Appl. Math*, **58** (2005), 579–619.
[16] T. F. Chan, J. Shen and H.-M. Zhou, Total variation wavelet inpainting, *Journal of Mathematical Imaging and Vision*, **25** (2006), 107–125.
[17] A. Criminisi, P. Pérez and K. Toyama, Region filling and object removal by exemplar-based image inpainting, *IEEE Transactions on Image Processing*, **13** (2004), 1200–1212.
[18] K. Dabov, A. Foi, V. Katkovnik and K. Egiazarian, Image denoising with block-matching and 3D filtering, in *Electronic Imaging 2006, International Society for Optics and Photonics*, (2006), 606414–606414.
[19] B. Dong, H. Ji, J. Li, Z. Shen and Y. Xu, Wavelet frame based blind image inpainting, *Applied and Computational Harmonic Analysis*, **32** (2012), 268–279.
[20] B. Dong and Z. Shen, MRA based wavelet frames and applications, *IAS Lecture Notes Series, Summer Program on "Mathematics of Image Processing"*, IAS/Park City Math. Ser., 19, Amer. Math. Soc., Providence, RI, 2013, 9–158.
[21] W. Dong, G. Shi, X. Li, Y. Ma and F. Huang, Compressive sensing via nonlocal low-rank regularization, *IEEE Transactions on Image Processing*, **23** (2014), 3618–3632.
[22] W. Dong, G. Shi and X. li, Nonlocal image restoration with bilateral variance estimation: A low-rank approach, *IEEE Transactions on Image Processing*, **22** (2013), 700–711.
[23] M. Elad, J.-L. Starck, P. Querre and D. L. Donoho, Simultaneous cartoon and texture image inpainting using morphological component analysis (MCA), *Applied and Computational Harmonic Analysis*, **19** (2005), 340–358.
[24] M. J. Fadili, J. L. Starck and F. Murtagh, Inpainting and zooming using sparse representations, *Comput. J.*, **52** (2009), 64–79.
[25] G. Gilboa and S. Osher, Nonlocal operators with applications to image processing, *Multiscale Model. Simul.*, **7** (2008), 1005–1028.
[26] G. Gilboa, N. Sochen and Y. Zeevi, Image enhancement and denoising by complex diffusion processes, *Pattern Analysis and Machine Intelligence*, IEEE Transactions on, **26** (2004), 1020–1036.
[27] G. Gilboa, N. Sochen and Y. Y. Zeevi, Forward-and-backward diffusion processes for adaptive image enhancement and denoising, *IEEE Transactions on Image Processing*, **11** (2002), 689–703.
[28] R. Glowinski and P. Le Tallec, *Augmented Lagrangian and Operator-Splitting Methods in Nonlinear Mechanics*, SIAM, 1989.
[29] H. Ji, Z. Shen, and Y. Xu, Wavelet frame based image restoration with missing/damaged pixels, *East Asia Journal on Applied Mathematics*, **1** (2011), 108–131.
[30] R. Lai and J. Li, Manifold based low-rank regularization for image restoration and semi-supervised learning, *Journal of Scientific Computing*, **74** (2018), 1241–1263.
[31] F. Li and T. Zeng, A universal variational framework for sparsity-based image inpainting, *IEEE Transactions on Image Processing*, **23** (2014), 4242–4254.
[32] T. März, Image inpainting based on coherence transport with adapted distance functions, *SIAM Journal on Imaging Sciences*, **4** (2011), 981–1000.
[33] A. Newson, A. Almansa, Y. Gousseau and P. Pérez, Non-local patch-based image inpainting, *IPOL J. Image Processing On Line*, **7** (2017), 373–385.
[34] S. Osher, Z. Shi and W. Zhu, Low dimensional manifold model for image processing, *SIAM Journal on Imaging Sciences*, **10** (2017), 1669–1690.
[35] A. Ron and Z. Shen, Affine Systems in $L_2(\mathbb{R}^d)$: The Analysis of the Analysis Operator, *Journal of Functional Analysis*, **148** (1997), 408–447.
[36] Z. Shen, Wavelet frames and image restorations, *Proceedings of the International Congress of Mathematicians*, Volume IV, Hindustan Book Agency, New Delhi, 2010, 2834–2863.
[37] Z. Shi, S. Osher and W. Zhu, Weighted graph laplacian and image inpainting, *Journal of Scientific Computing*, **577** (2017).
[38] J. Yu, Z. Lin, J. Yang, X. Shen, X. Lu and T. Huang, Generative image inpainting with contextual attention, **06** (2018), 5505–5514.

[39] K. Zhang, W. Zuo, Y. Chen, D. Meng and L. Zhang, Beyond a gaussian denoiser: Residual learning of deep cnn for image denoising, *IEEE Transactions on Image Processing*, **26** (2017), 3142–3155.

Received April 2020; 1st revision August 2020; final revision November 2020.

E-mail address: chenyt96@mail3.sysu.edu.cn
E-mail address: lijia66@mail.sysu.edu.cn
E-mail address: yuqy8@mail2.sysu.edu.cn